The International Journal of Artificial Organs / Vol. 29 / no. 2, 2006 / pp. 239-250

Biomaterials

Multi-scale analysis of the Toraymyxin adsorption cartridge Part I: Molecular interaction of polymyxin B with endotoxins

S. VESENTINI, M. SONCINI, A. ZAUPA, V. SILVESTRI, G.B. FIORE, A. REDAELLI

Department of Bioengineering, Politecnico di Milano, Milan - Italy

ABSTRACT: Endotoxins or lipopolysaccharides are the main constituents of the outer leaflet of Gram-negative bacteria membrane and play a central role in the pathogenesis of the septic shock. Polymyxin B has both antibacterial and antiendotoxin capability; indeed it is able to destroy the bacterial outer membrane and bind endotoxin neutralizing its toxic effects. Cartridges containing polymyxin B-immobilized fibers (Toraymyxin PMX-F, Toray Industries, Japan) are used in extracorporeal hemoperfusion to remove circulating endotoxin.

The aim of this study is the characterization of the polymyxin B-endotoxin system at the molecular level, thus providing quantitative evaluation of the binding forces exerted in the molecular complex.

Polymyxin B was interfaced with five molecular models of lipopolysaccharides differing in their structure and molecular mechanics simulations were performed at different intermolecular distances aimed at calculating the interaction energies of the complex. Binding forces were calculated by fitting interaction energies data.

Results show that in the short range the polymyxin B-endotoxin complex is mediated by hydrophobic forces and in the long range the complex is driven by ionic forces only. From a mechanical standpoint, polymyxin B-endotoxin complex is characterized by maximum binding forces ranging between 1.39 nN to 3.79 nN. The knowledge of the binding force behavior at different intermolecular distances allows further investigations at higher scale level (Part II). (Int J Artif Organs 2006; 29: 239-50)

KEY WORDS: Sepsis, Polymyxin B, Lipopolysaccharide, Endotoxins, Molecular interaction, Molecular modelling

INTRODUCTION

Sepsis is a generalized infection of the organism, supported by the presence of bacteria in blood (bacteremia). An effective defence of the host against bacteremia requires the functionality of circulating macrophages and phagocytes, otherwise the permanence of bacteria in the blood stream leads to a generalized infection. Recently, clinical and scientific research has been focused on endotoxinic therapies, acting directly on endotoxins, which are the main constituent of the outer leaflet of Gram-negative bacteria external membrane and are a trigger of the inflammatory process.

Antiendotoxin strategies proposed in clinical trials such as monoclonal antibodies, antiendotoxin vaccines, and inhibitor agents of endotoxin synthesis did not achieve reproducible results in terms of benefit in the clinical status of septic patients probably due to weak and not specific bond achieved in the complex with the lipid tail of endotoxin (1). In this field, an interesting antiendotoxin strategy is represented by Toraymyxin cartridge (Toraymyxin PMX-F, Toray Industries, Japan), an external

© Wichtig Editore, 2006

0391-3988/239-12 $15.00/0

device able to provide selective removal of endotoxins. Toraymyxin filter is a cartridge containing the antibiotic polymyxin B (PMB), a cationic amphiphilic cyclic decapeptide able to destroy the bacterial membrane (antibacterial effect) and to bind the residual endotoxins (antiendotoxin effect).

It is well known that PMB neutralizes the toxic effects of endotoxins, but its nephrotoxic and neurotoxic effects have been widely demonstrated, when PMB is released both at local and systemic levels (2). In the Toraymyxin device, PMB is covalently grafted on the fiber surface, a knitted tissue of polypropylene and α-chloroacetamide-methylpolystyrene, thus avoiding the negative effects produced by circulating PMB. Clinical trials on Toraymyxin cartridge demonstrated that the survival rate of patients with sepsis increases (3-6).

From a chemical point of view, endotoxins are lipopolysaccharides (LPS) constituted by a hydrophilic polysaccharide domain bound to a hydrophobic lipid tail (lipid A), which is the LPS portion embedded in the bacterial outer membrane (Fig. 1a). Lipid A consists of a diphosphorylated D-glucosamine disaccharide backbone acylated by up to seven asymmetric fatty acid chains. The polysaccharide region consists of a sequence of oligosaccharide units (O-antigen) and several rare sugars (inner and outer core). The structure of the O-antigen varies markedly among different bacterial species and provides serotype specificity and polar properties to the overall LPS structure. In turn, the core portion shows slight inter-bacterial variability; the lipid A portion is the more conserved structure in LPS and it is responsible for most of the pathological effects (7-9).

In physiologic conditions, the LPS structure is highly amphiphilic. The expression of endotoxic activity is due to a specific equilibrium between hydrophilic (diphosphorylated disaccharide backbone and ionization state of phosphate groups) and hydrophobic (number, length and position of fatty acid chains) regions to achieve an active state. This conformation is promoted by the 2-keto-3deoxy-manno-octonoic acid dimer (Kdo) of the inner-core directly connected to the lipid-A saccharide backbone (10, 11). In the Kdo-Kdo-lipid A complex named ReLPS (Fig. 1b) the Kdo negative charges play a regulatory effect on the ionization state of disaccharide backbone, which influences the fatty acid chain configuration.

One antiendotoxin strategy consists in the removal of LPS throughout lipid A binding agents, in order to prevent LPS interactions with specific immune system receptors. PMB, shown in Figure 2, is able to specifically bind the lipid-A region and to compromise the spatial organization of the fatty acid chains, thus neutralizing LPS toxic effects. PMB is a highly amphiphilic molecule due to the presence of hydrophobic groups alternating with hydrophilic positively charged diaminobutirric acid (Dab) residues (12).

Several studies have revealed that the amphiphilic nature of LPS and PMB is responsible for their interaction (12-14). In particular, the interaction between PMB and LPS complex is based both on ionic and hydrophobic forces. At first, the phosphate groups, with negative charge of lipid A, interact with positively charged Dab residues of PMB with a 1:2 ratio (2, 12-15). This event, driven by ionic forces, promotes the second step of the bond stabilization, which is characterized by hydrophobic contacts between fatty acid chains of the lipid A and PMB hydrophobic residues.

The present work focuses on the investigation of the interaction forces generated in LPS-PMB complexes. To reach this goal five different molecular models of LPS structures were constructed and the interaction forces between LPSs and PMB at different distances were calculated by means of the molecular mechanics approach. The study at the molecular level is the first step to assess the mechanisms underlying the ability for the Toraymixin device in capturing endotoxins from the blood stream (Part II).

METHODS

The molecular models of PMB and five different LPS structures were developed. Two different large endotoxins and three endotoxin precursors were considered. Molecular mechanics simulations were then performed in order to calculate the interaction forces. The molecular models and the molecular analyses were developed with the computational chemistry commercial package Hyperchem 6.01 (Hyperchem®, Hypercube, Canada) using the force field Amber 3, specific for biological molecule treatment, and a dielectric constant equal to 78 to simulate an implicit water-like environment.

LPS models

In this work five LPS structures were developed; firstly, the complete endotoxin structure (S-LPS) (Fig. 1a) and the

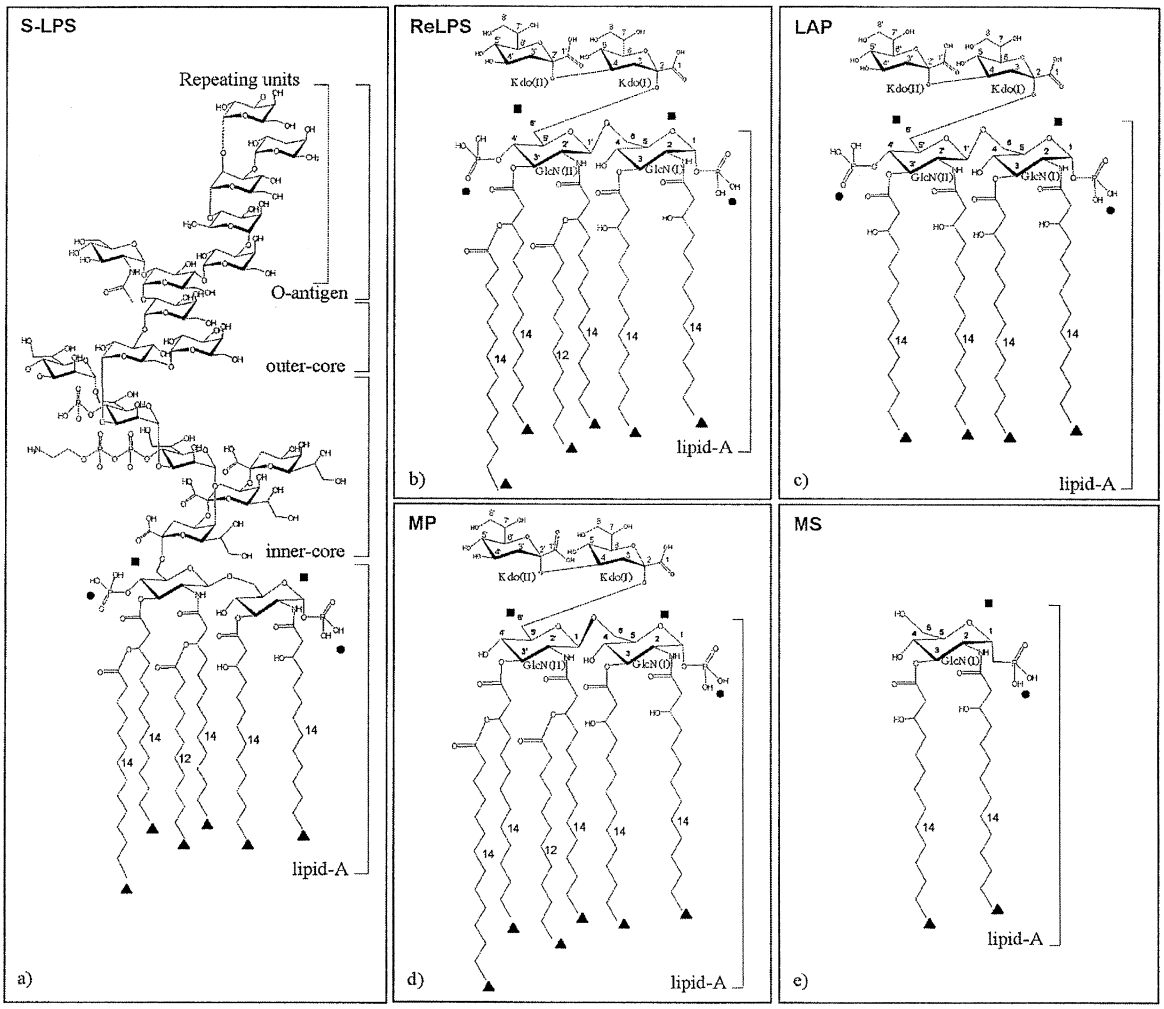

Fig. 1 - *Chemical structure of lipopolysaccharides.* **(a)** *S-LPS molecule (S-LPS), where O-antigen, outer-core, inner-core and lipid A are highlighted.* **(b)** *Structure of ReLPS (ReLPS), which consists of lipid A (composed of a D-glucosamine disaccharide with two phosphate groups attached to position 1 and 4' - GlcN(I) and GlcN(II) and by six fatty acid residues linked to the saccharide backbone) and inner-core region (composed of the α-(2, 4)-dimer of 2-keto-3deoxy-manno-octonoic acid, named Kdo-Kdo group).* **(c)** *Primary structure of the precursor of lipid A (LAP), derived from ReLPS model without fatty acid side secondary chains.* **(d)** *Structure of ReLPS monophosphate (MP), without phosphate group at the position 4 (GlcN(II)).* **(e)** *ReLPS monosaccharide (MS), without one of the sugars of its saccharide backbone (GlcN(II)) and related fatty acid chains and Kdo-Kdo group. In all the reported chemical structures the fatty acid chains are indicated by ▲, phosphate groups by ● and sugar group by ■. Numbers close to the fatty acid chains indicate the number of carbon atoms.*

minimum structure needed to accomplish the lipopolysaccharide endotoxin activity which is the Kdo-Kdo-lipid A complex (ReLPS) (Fig. 1b). Subsequently, in order to evaluate the effects of ionic and hydrophobic interactions, achieved in the molecular complex, three other structures were obtained by further removing some functional groups from the ReLPS. In particular, the lipid-A precursor (LAP) was obtained from ReLPS by removing the secondary fatty acid chains (Fig. 1c), thus reducing the hydrophobic interaction; the monophosphate precursor (MP) was

obtained by eliminating the phosphate group in position 4 (Fig. 1d), thus reducing the ionic interaction; the monosaccharide (MS) was obtained by removing an entire sugar from its saccharide backbone, and the corresponding phosphate group and fatty acid chains (Fig. 1e), thus reducing both ionic and hydrophobic interaction.

The ReLPS and S-LPS models were obtained according to atomic models proposed by Kastowsky and co-workers (10).

Atomic charges were calculated using the Gasteiger and Marsili method (16) based on partial equalization of orbital electronegativity scheme, which assigns charges depending on the atom hybridization state. The ionization state of the ReLPS molecular model was assigned according to Din and co-workers (15), reporting four negative charges per monomer at physiological pH. Negative charges are located on the two phosphate groups of lipid A and on the two carboxylate groups of Kdos. To each phosphate group a charge of -1e (e is the electron charge equal to $1.6 \cdot 10^{-19}$ C) was assigned, equally shared among the three oxygen atoms of the group. An atomic charge of -0.5e was imposed for the two oxygens of the carboxylic groups in the Kdo. The ionization state of S-LPS molecular model was assigned according to atomic charges used for the Kdo-Kdo-lipid A portion in the ReLPS model and the third Kdo residue was assigned following the same criterion adopted for the other two Kdo residues.

The S-LPS and ReLPS models were optimized using first the steepest-descent and afterwards the Polak-Ribiere minimization algorithms, in order to obtain the initial configuration corresponding to the minimum potential energy of the molecular system. Combining these two minimization algorithms leads to a satisfying optimization procedure saving computational costs.

The LAP, MP, MS models were derived from the optimized ReLPS model, maintaining the ionization state; they were optimized following the same optimization procedure adopted for large complexes.

PMB model

The active PMB structure was obtained starting from the atomic coordinates by Pristovsek and Kidric (12). This structure represents PMB molecule in the typical conformation bound to the lipid-A region of endotoxins. Atomic charges were calculated using the Gasteiger and Marsili empiric method (16). A total charge of +0.5e was assigned for the amine group (NH_2) of each Dab residue, equally shared between the two hydrogen atoms. In order to preserve the bound conformation of the PMB model (12), the molecular structure was not optimized in water-like environment. In this way the model maintains its highly amphiphilic conformation with the hydrophobic residues laying on the left side of a plane π and the hydrophilic residues laying on the opposite side (Fig. 2b). In this configuration the distance between the center of mass of Dab1-Dab5 group (Fig. 2b) and the center of mass of Dab8-Dab9 is 1.15 nm (Fig. 2c). The total length of the molecule is 2.6 nm.

LPS-PMB interaction

Five different complexes ($C_{S\text{-}LPS}$, C_{ReLPS}, C_{LAP}, C_{MP}, C_{MS}) were prepared coupling the five endotoxin models (S-LPS, ReLPS, LAP, MP, MS) with the PMB molecular model. To obtain a proper interaction between the two molecular systems involved in the complex, the positive Dab residues of PMB (Dab1-Dab5 and Dab8-Dab9) were faced to the negative phosphate groups of the glicolipids GlcN I and GlcN II in the lipid A portion of the related LPS model.

In addition, concerning $C_{S\text{-}LPS}$ and C_{ReLPS} complexes, two different ways of facing were considered (Fig. 3). Indeed the way that the LPSs move towards the PMB chemically bound to the fiber surface is not univocal. Two different ways of facing allow simulating two different approach modes: the first one with Dab1-Dab5 residue faced to GlcN I phosphate group and Dab8-Dab9 residue faced to GlcN II ($C_{S\text{-}LPS(I)}$, $C_{ReLPS(I)}$), (Figs. 3a and 3c), and the second one with Dab1-Dab5 residue faced to GlcN II phosphate group and Dab8-Dab9 residue faced to GlcN I ($C_{S\text{-}LPS(II)}$, $C_{ReLPS(II)}$), (Figs. 3b and 3d). In both cases the two molecules interact through their hydrophobic groups.

The energy optimization of all the complex models was performed to obtain a stable coupling between PMB and LPS. The following procedure was adopted: i) optimization of the entire molecular system; ii) application of restraints between the H atom of the aminic group in the Dab and the O atom of the phosphate group, in order to promote the hydrogen bond formation; to reach this goal OH distance was set equal to 2 Å and OHN angle equal to 180 degrees, according to literature data (12); iii) optimization of the entire molecular system with restraints activated; iv) optimization of the entire molecular system with the restraints released and both molecules free to move.

The optimized complexes obtained with this procedure

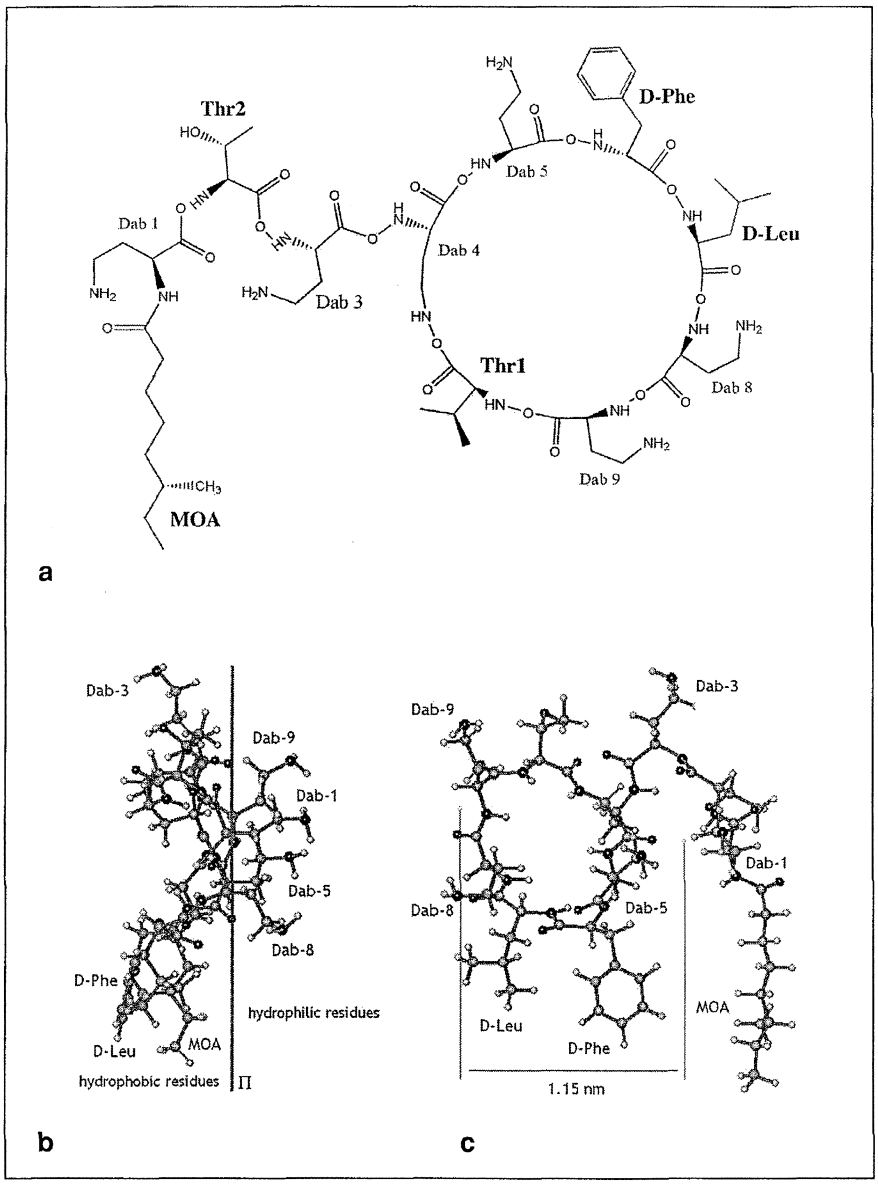

Fig. 2 - *Chemical structure of polymixyne B* **(a)**. *Molecular structure of PMB: the amphiphilic nature of PMB molecule is represented; the hydrophilic residues (Dab1, Dab5, Dab8 and Dab9) and the hydrophobic groups (D-Phe, D-Leu and the metil-octanoic acid MOA) lay on opposite sides of* π *plane* **(b)**. *The distance between the center of mass of the two hydrophilic groups which are involved in the complex formation (Dab1-Dab5 and Dab8-Dab9) is reported* **(c)**.

were then used as initial configurations for the simulations at different intermolecular distances. Intermolecular distance was imposed on the molecular system moving the LPS molecule toward or apart from the PMB and the complex was optimized in two steps to achieve the minimum energy configuration. In particular, in the first step PMB structure is fixed and LPS is free to move, in the second step both molecules are free to move. The single reaction coordinate r_{PL} was imposed by moving the LPS center of mass (CM_L) with respect to the PMB center of

mass (CM_P) along the line connecting CM_L and CM_P by 0.05 nm. Namely, r_{PL} represents the intermolecular distance and it was calculated as:

$$r_{PL} = \sqrt{(x_{CM_P} - x_{CM_L})^2 + (y_{CM_P} - y_{CM_L})^2 + (z_{CM_P} - z_{CM_L})^2} \quad [1]$$

$$x_{CM} = \frac{\sum_k m_k x_k}{\sum_k m_k}; \qquad y_{CM} = \frac{\sum_k m_k y_k}{\sum_k m_k}; \qquad z_{CM} = \frac{\sum_k m_k z_k}{\sum_k m_k} \quad [2]$$

where x_k, y_k, z_k are the atomic spatial coordinates and m_k is the atomic weight of each atom k.

For each applied intermolecular distance, the interaction energy (E'_{PL}) was obtained by subtracting the potential energy of the PMB (E_P) and the LPS (E_L) to the potential energy of the overall system (E_{TOT}):

$$E'_{PL} = E_{TOT} - E_P - E_L \quad [3]$$

E'_{PE} values, calculated by Eq. [3], were then interpolated using a Lennard-Jones (L-J) potential, which represents the interaction energy (E_{PL}) between the two molecules as a function of the intermolecular distance (r_{PL}):

$$E_{PL} = 4\varepsilon\left[\left(\frac{\sigma}{r_{PL}}\right)^{12} - \left(\frac{\sigma}{r_{PL}}\right)^{6}\right] \quad [4]$$

where ε and σ are the L-J parameters determined through a best-fit algorithm. These parameters represent physical properties of the molecular system; in particular, ε represents the equilibrium energy ($E_{PLmin} = \varepsilon$) and σ the equilibrium length ($r_{PLmin} = \sigma \bullet 2^{1/6}$).

The binding force is calculated as the first order derivative of the interaction energy (E_{PL}) with respect to the intermolecular distance (r_{PL}):

$$F(r_{PL}) = -\frac{dE_{PL}}{dr_{PL}} = 24\varepsilon\left[2\frac{\sigma^{12}}{r_{PL}^{13}} - \frac{\sigma^6}{r_{PL}^7}\right] \quad [5]$$

RESULTS

In order to characterize the nature of the interactions that each LPS molecular structure can potentially accomplish with PMB, two parameters were considered: the distance between the two phosphate groups ($\delta_{P\text{-}P}$) and the hydrophobic surface accessible to the solvent (HSAS). Namely the first parameter is related to the ionic effect, whereas HSAS is related to the hydrophobic effect. Data related to potential energy (E_P), $\delta_{P\text{-}P}$ and HSAS are reported in Table I for each LPS model and are referred to the endotoxin configuration after energy optimization in a water-like environment. The van der Waals volume was calculated for large LPSs: 5.11 nm^3 for ReLPS and 16.02 nm^3 for S-LPS.

As for LPS-PMB complexes, the energy and structural data are collected in Table II. The main contribution of the interaction energy is due to hydrophobic effect (E_{vdW} = 96-98%); except for C_{MS} complex (E_{vdW} = 44%), which is characterized by the lowest number of fatty acid chains (Tab. II, column 3). From a stereo-specific point of view, the interaction due to the ionic effect can be evaluated by the comparison of the LPS distance $\delta_{P\text{-}P}$ with the PMB distance $\delta_{D\text{-}D}$ between the two Dab residual pairs (Tab. II, Columns 5 and 6). After energy minimization, complexes with large endotoxins ($C_{S\text{-}LPS(I)}$, $C_{S\text{-}LPS(II)}$, $C_{ReLPS(I)}$, $C_{ReLPS(II)}$) show a very small mismatch between Dab and phosphate group positions (0.04 nm), which is comparable with the mismatch of the initial configuration ($\delta_{P\text{-}P}$ = 1.20 nm and $\delta_{D\text{-}D}$ = 1.15 nm) referred to an active bound complex (10, 12). A different behavior was observed for complexes with precursors, which show a greater mismatch (0.3 nm for C_{LAP} and C_{MP} and 0.06 nm for C_{MS}) due to geometrical differences determined by the removal of groups in the LPS molecular structure. The lack of specific regions in the LPS structure induces conformational changes of PMB, which causes the molecule to shrink and consequently reduces the distance between the center of mass of Dab groups.

TABLE I - ENERGETIC AND GEOMETRICAL PARAMETERS CALCULATED FOR THE FIVE CONSIDERED LPS MODELS AFTER OPTIMIZATION PROCESS

LPS model	E_{TOT} [kJ/mol]	$\delta_{P\text{-}P}$ [nm]	HSAS [nm^2]
S-LPS	-785	1.22	14.96
ReLPS	-78	1.22	14.89
LAP	-105	1.20	13.66
MP	-102	-*	19.31
MS	-44	-*	10.06

E_{TOT}, total potential energy of the molecular system; $\delta_{P\text{-}P}$, distance between the two phosphate groups; HSAS, hydrophobic surface available to the solvent; *only one phosphate group is present within the LPS molecule.

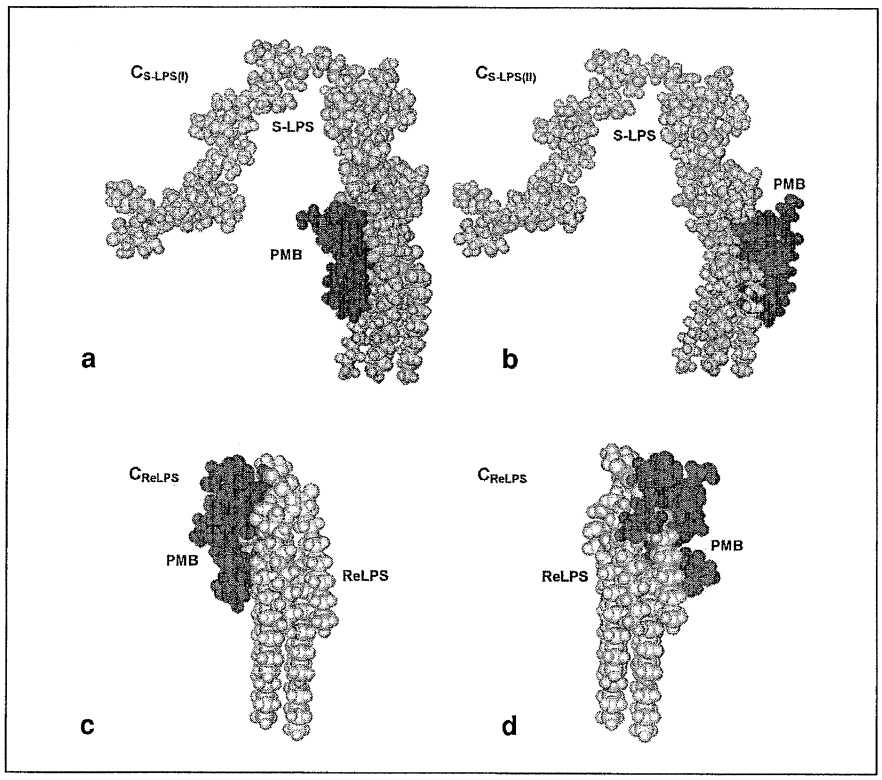

Fig. 3 - *Different ways of facing of S-LPS and PMB in $C_{S\text{-}LPS}$ complex* **(a, b)** *and of ReLPS and PMB in C_{ReLPS} complex (c, d). Dab1-Dab5 residue are faced to GlcN I phosphate group and Dab8-Dab9 residue faced to GlcN II* **(a, c)**; *Dab1-Dab5 residue faced to GlcN II phosphate group and Dab8-Dab9 residue faced to GlcN I* **(b, d)**.

This behavior is markedly evident for the C_{MS} complex.

The interaction energy was evaluated for all seven complexes in order to quantify the L-J binding energy curve and consequently the force. The distance between the centers of mass of PMB and LPS (r_{PL}) was changed as reported in the Methods Section and the interaction energy (E'_{PL}) was calculated as a function of r_{PL}. Figure 4 shows the E'_{PL} values obtained for the complexes with large endotoxins ($C_{S\text{-}LPS(I)}$, $C_{S\text{-}LPS(II)}$, $C_{ReLPS(I)}$, $C_{ReLPS(II)}$) and Figure 5 shows the E'_{PL} data obtained for precursor LPS complexes (C_{LAP}, C_{MP}, C_{MS}).

The high mobility of the LPS molecule, particularly in

TABLE II - ENERGETIC AND GEOMETRICAL PARAMETERS CALCULATED FOR THE SEVEN CONSIDERED LPS-PMB COMPLEXES AFTER OPTIMIZATION PROCESS

LPS-PMB complex	E'_{PL} [kJ/mol]	E_{vdW} [%]	E_{el} [%]	$\delta_{P\text{-}P}$ [nm]	$\delta_{D\text{-}D}$ [nm]	HSAS [nm²]
$C_{S\text{-}LPS(I)}$	-264	97	3	1.23	1.19	12.25
$C_{S\text{-}LPS(II)}$	-308	97	3	1.21	1.2	12.07
$C_{ReLPS(I)}$	-247	96	4	1.19	1.18	12.55
$C_{ReLPS(II)}$	-231	96	4	1.16	1.2	12.76
C_{LAP}	-178	96	4	1.16	0.85	11.44
C_{MP}	-233	98	2	-*	0.87	12.73
C_{MS}	-165	44	56	-*	0.44	7.01

E'_{PL}, interaction energy of the molecular complex; E_{vdW}, van der Waals energy; E_{el}, electrostatic energy; $\delta_{P\text{-}P}$, distance between the two phosphate groups; $\delta_{D\text{-}D}$, distance between the center of mass of the two Dab groups in PMB; HSAS, hydrophobic surface available to the solvent; *only one phosphate group is present within the LPS molecule.

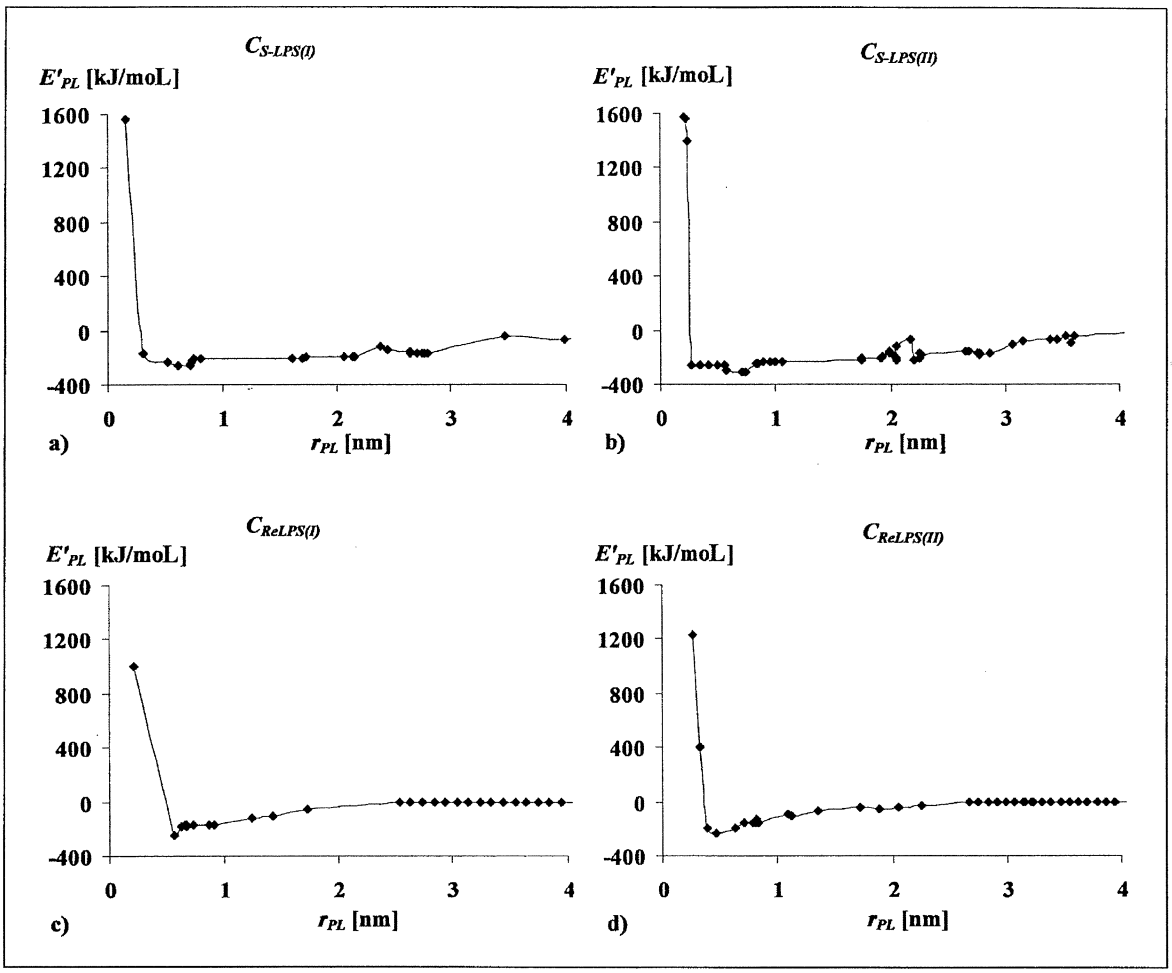

Fig. 4 - *Interaction energy vs. intermolecular distance obtained for complexes with large endotoxins differently faced:* $C_{S\text{-}LPS(I)}$ **(a)**, $C_{S\text{-}LPS(II)}$ **(b)**, $C_{ReLPS(I)}$ **(c)**, $C_{ReLPS(II)}$ **(d)**.

TABLE III - BINDING FORCE AND RELATED L-J CURVE PARAMETERS OBTAINED FOR THE LPS-PMB COMPLEXES

LPS-PMB complex	F_{max} [nN]	ε [kJ/mol]	σ [nm]
$C_{S\text{-}LPS(I)}$	1.05 ± 0.89	247.0 ± 15.0	0.54 ± 0.08
$C_{S\text{-}LPS(II)}$	2.69 ± 1.10	274.0 ± 33.0	0.63 ± 0.13
$C_{ReLPS(I)}$	1.02 ± 0.94	209.0 ± 38.0	0.65 ± 0.15
$C_{ReLPS(II)}$	1.13 ± 1.04	196.0 ± 35.0	0.58 ± 0.16
C_{LAP}	0.98 ± 0.41	156.3 ± 21.8	0.72 ± 0.21
C_{MP}	1.28 ± 0.57	222.5 ± 10.7	0.41 ± 0.14
C_{MS}	0.96 ± 0.84	132.9 ± 31.7	0.46 ± 0.10

F_{max}, maximum binding force; ε, equilibrium energy; σ, equilibrium length.

large structures such as S-LPS and ReLPS, made meaningless the use of a single L-J curve to describe this behavior. In fact the low energy region, which extends from 0.5 to 1 nm, is likely due to the presence of different distances of minimum energy. Consequently three different L-J curves were calculated for each complex and a parameter range was obtained as shown in Table III (Columns 2 and 3). Using these values and calculating the first derivative of the L-J curves Eq. [5], the binding force as a function of the intermolecular distance was obtained. A range of maximum force values for each complex is reported in Table III (Column 1).

Considering both large complexes ($C_{S\text{-}LPS}$ and C_{ReLPS}) in both facing manner ($C_{S\text{-}LPS(I)}$, $C_{S\text{-}LPS(II)}$, $C_{ReLPS(I)}$ and $C_{ReLPS(II)}$), $C_{S\text{-}LPS}$ binding forces are higher than C_{ReLPS} (1.05 vs. 1.02 nN in first facing manner and 2.69 vs. 1.13 nN in second facing manner). Furthermore, the second facing mode shows to be stronger than the first one in both complexes (2.69 vs 1.05 nN for $C_{S\text{-}LPS}$ and 1.13 vs 1.02 nN for C_{ReLPS}). Convincingly, large complexes show binding forces slightly higher than small complexes, where some functional groups have been removed (Tab. III, column 1). Differences will be examined in detail in the Discussion section.

Finally, Figure 6 represents snapshots of the ReLPS-PMB complex at different interaction distances. For each configuration simulated, the intermolecular distance and the maximum binding force (calculated with σ = 0.74 nm and ε = 231 kJ/mol) are also reported. In Figure 6, the short range (A, B and C) and the long range (D-H) conformations are represented. In the short range, the fatty acid chains stabilize the complex and the resulting binding force is about 2nN due to both ionic and hydrophobic effects; in the long range, when the distance between molecules is progressively increased, ionic forces become prevalent and the binding force decreases up to three orders of magnitude.

DISCUSSION

At the molecular level the effectiveness of antiendotoxin treatments, based on the specific interaction between endotoxin and PMB molecules, is due to the formation of a stable and a specific bond between these two actors. It is well known that PMB neutralizes toxic effects of endotoxins by forming a specific and high effective endotoxin-antibiotic complex. In recent years, concerning LPS-PMB interaction, two different chemical mechanisms

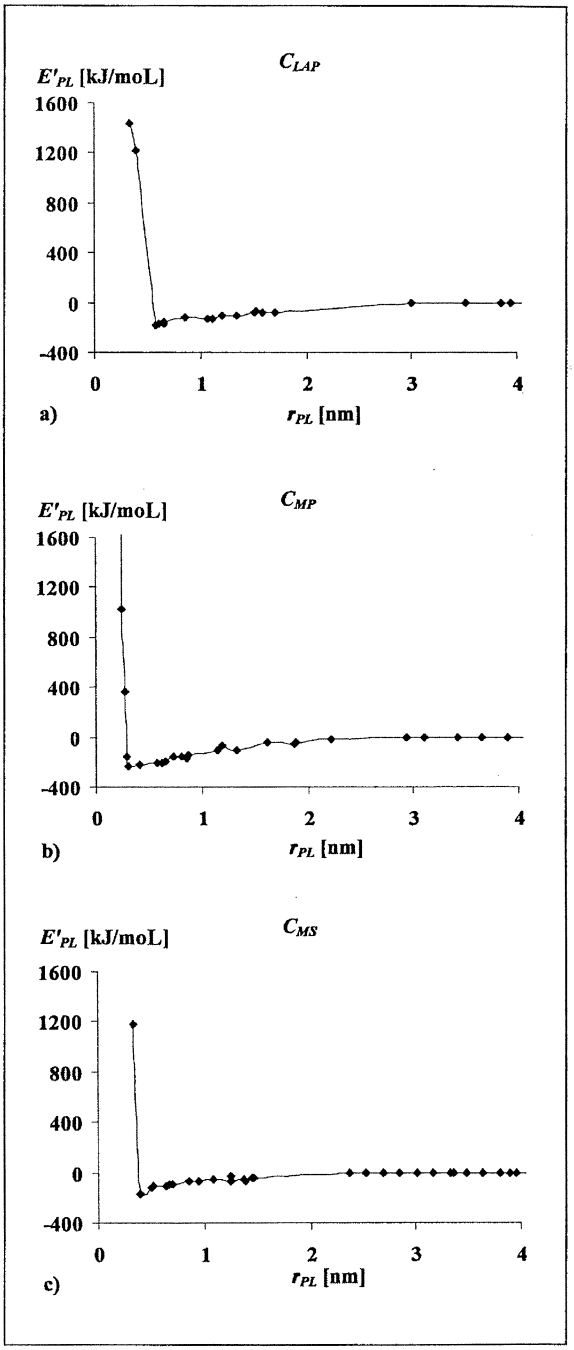

Fig. 5 - *Interaction energy vs. intermolecular distance obtained for complexes with endotoxin precursors:* C_{LAP} **(a)**, C_{MP} **(b)**, C_{MS} **(c)**.

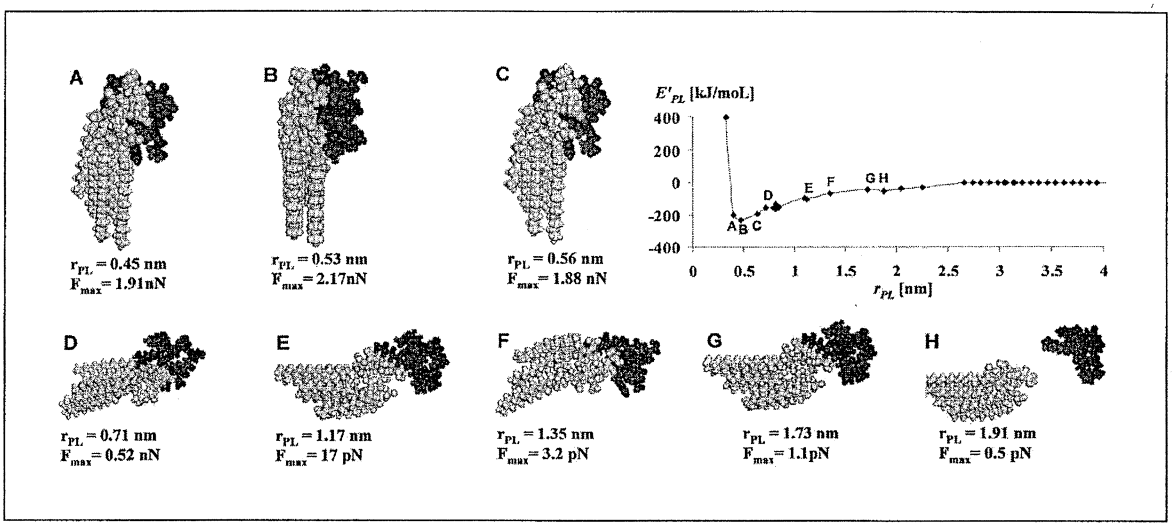

Fig. 6 - *Sequence of configurations explored by the molecular complex $C_{ReLPS(II)}$ during the simulation performed at different intermolecular distances. In the short range configurations represented by snapshots A, B and C (low intermolecular distances and high binding forces) the interaction between PMB and LPS is related to both ionic and hydrophobic effects; in the long range configurations represented by snapshots from D to H the interaction is driven by ionic effect only (smaller binding forces).*

have been proposed to drive and to stabilize this complex: ionic and hydrophobic (12). The purpose of the present work was to point out and quantify which character, ionic or hydrophobic, is predominant in the short and long ranges by means of molecular mechanics simulations. Furthermore, interaction energies as a function of intermolecular distance between PMB and LPS molecules were obtained and subsequently used to calculate the binding force at the molecular level. Two different interfaces were also considered ($C_{S\text{-}LPS(I)}$, $C_{S\text{-}LPS(II)}$ and $C_{ReLPS(I)}$, $C_{ReLPS(II)}$) in order to take into account the arbitrary character for complex formation. Indeed it is well known that LPS and PMB interact with each other via their phosphate and Dab groups respectively but two conformations can be realized (Fig. 3).

Our results show that in the short range (intermolecular distances in the range 0.4-0.9 nm) the hydrophobic contact and linkage between lipid A fatty acid chains of LPS and PMB hydrophobic residues (12-14) stabilize the complex. In the long range (intermolecular distances higher than 1nm) LPS phosphate groups, with negative charge, interact with positively charged Dab residues of PMB (2, 12-15) thus giving rise to ionic interactions. Indeed it is possible to disclose that the ionic part, within the LPS, moves toward the ionic site of PMB and successively the hydrophobic sites of both molecules approach each other in order to reduce the hydrophobic surface accessible to the solvent (comparison between Tab. II, column 7 and Tab. I, column 4). Accordingly, complexes with a lower number of fatty acid chains (C_{LAP} and C_{MS}) show lower interaction. This behavior is in agreement with the hypothesis that hydrophobic forces play a key role in the short range and ionic force is the predominant term in the long range interaction (2, 14, 17).

Binding forces calculated for $C_{S\text{-}LPS}$ are higher than those observed for C_{ReLPS}. This is probably due to the fact that the saccharidic portion of S-LPS is larger than the corresponding portion within ReLPS. Also complexes with LPS precursors (C_{LAP}, C_{MP}, C_{MS}) were studied in order to estimate which groups, within the LPS, would influence the interaction with PMB and consequently would show the largest binding force. Concerning Table III it is possible to draw some remarks. The values calculated for the maximum binding force are greater than those referred to small complexes: this is definitely due to the suppression of functional groups in the small LPSs. The difference is wide for C_{LAP} and C_{MS} whereas for C_{MP} the difference is negligible. This is likely related to the number of fatty acid chains within LPSs. S-LPS, ReLPS and MP have six fatty acid chains whereas LAP and MS have four and two fatty

acid chains, respectively. The highest binding interactions are detected for $C_{S\text{-}LPS}$ and C_{ReLPS} complexes which are those containing the complete structure of lipid A as proposed by Yin and co-workers (14). Their maximum binding force ranges between 1.94 nN and 3.79 nN whereas it ranges between 1.39 nN and 1.85 nN for the other three complexes (C_{LAP}, C_{MP} and C_{MS}). Data obtained for the binding force generated in the LPS-PMB complexes are of the same order of magnitude as, but higher than, literature data obtained by means of atomic force microscopy concerning: i) the antigen-antibody complex (0.1-0.05 nN) (18); ii) the protein complex involved in cell adhesion (0.4 nN) (19); iii) the complex involving the receptor protein of *Escherichia Coli Bacterium* and its proteic substrate (0.4-0.9 nN) (20). This comparison makes it possible to state that LPSs, both in large and precursor structures, are able to establish very stable complexes with PMB, generating higher binding forces than other common biological complexes.

The influence of the hydrophobic term in the short range interaction can be evaluated by calculating the van der Waals component within the interaction energy. In all complexes at minimum energy level (data in Tab. II) the van der Waals terms account for up to 96-98% thus supporting that the bond stabilization is based on hydrophobic forces. Only for C_{MS} the van der Waals term, which accounts for 44%, is lower than the ionic term. Indeed, MS has only two fatty acid chains and, accordingly, C_{MS} exhibits the lowest interaction energy and the van der Waals term (E_{vdW}) and the ionic term (E_{el}) have similar relevance. The hydrophobic effect is also evident comparing the HSASs calculated for the optimized LPSs (Tab. I, column 4) and the HSASs calculated for the LPS-PMB complexes at minimum energy level (Tab. II, column 7). In all cases HSASs decrease when the complex is formed, that is LPS and PMB face each other in order to reduce the fatty acid surface in contact to the water-like environment. Furthermore the importance of the hydrophobic term in the short range is also confirmed by the comparison of interaction energies between the C_{MP} and the C_{ReLPS} complexes. Indeed, from a structural point of view, C_{MP} and C_{ReLPS} complexes have the same hydrophobic chains and similar minimum energy, but C_{MP} has only one phosphate group, consequently the phosphate group number (the ionic term) is less effective than hydrophobic chains.

In the present study all complexes were studied using the molecular mechanics approach. In order to reduce computational costs the water-like environment was simplified and the continuum implicit method was used. Indeed, the use of explicit solvent would produce a more realistic hydrogen bond pattern and probably influence both ionic and hydrophobic effects thus slightly increasing the binding force here calculated.

In order to quantify the effectiveness of Toraymyxin device at the molecular level two systems have to be considered: polypropylene and α-chloroacetamide-methylpolystyrene surface-PMB and LPS-PMB. Concerning the first system, PMB is covalently grafted on the fiber surface, thus preserving the patient from nephrotoxic and neurotoxic effects of PMB. Concerning the second system, the LPS-PMB complex interacts with ionic and hydrophobic forces which are weaker than direct covalent bond. Consequently in the present work our choice was to study only the weakest system, that is the LPS-PMB complex. From a multiscale point of view, it is possible to use the quantitative information on molecular interactions to set up dynamic simulation at higher scale level, namely at the micro-scale, taking the fluid-dynamic field within the Toraymyxin device into consideration. In particular it will be possible to investigate the competition between the drag forces exerted on LPS by fluid flow and binding forces exerted by PMB (Part II).

ACKNOWLEDGEMENTS

The authors thank Dr. P. Pristovsek of the National Institute of Chemistry, Ljubljana, Slovenia for having provided the atomic coordinates of polymyxin B and Dr. M.J. Kastowsky of the Max Planck Institute, Jena, Germany for having provided the atomic coordinates of S-LPS and ReLPS lipopolysaccharides.

Address for correspondence:
Ing. Monica Soncini, PhD
Department of Bioengineering
Politecnico di Milano
Piazza Leonardo da Vinci, 32
20133 Milano, Italy
e-mail: monica.soncini@polimi.it

REFERENCES

1. Opal SM, Glück T. Endotoxin as a drug target. Crit Care Med 2003; 31 (suppl): S57-64.
2. Morrison DC, Jacobs DM. Binding of polymyxin B to the lipid A portion of bacterial lipopolysaccharides. Immunochemistry 1976; 13: 813-8.
3. Hanasawa K, Aoki H, Yoshioka T, Matsuda K, Tani T, Kodama M. Novel mechanical assistance in the treatment of endotoxic and septicemic shock. ASAIO Trans 1989; 35: 341-3.
4. Shoji H, Tani T, Hanasawa K, Kodama M. Extracorporeal endotoxin removal by polymyxin B immobilized fiber cartridge: Designing and antiendotoxin efficacy in the clinical application. Ther Apher 1998; 2: 3-12.
5. Tani T, Hanasawa K. Therapeutic apheresis septic patients with organ dysfunction: Hemoperfusion using a polymyxin B immobilized column. Artif Organs 1998; 22: 1038-44.
6. Ebihara I, Nakamura T, Shimada N, Shoji H, Koide H. Effect of hemoperfusion with polymyxin B-immobilized fiber on plasma endothelin-1 and endothelin-1 mRNA in monocytes from patients with sepsis. Am J Kidney Dis 1998; 32: 953-61.
7. Brade H, Brade L, Rietschel ET. Structure-activity relationships of bacterial lipopolysaccharides (endotoxins). Current and future aspects. Zentralbl Bakteriol Mikrobiol Hyg [A] 1988; 268: 151-79.
8. Rietschel ET, Brade L, Schade U, Seydel U, Zäringer U, Kusumoto S, Brade H. Bacterial endotoxins: Properties and structure of biologically active domains. In: Schrinner E, Richmond MH, Seibert G, Schwarz U, eds. Surface structures of microorganisms and their interactions with the mammalian host. Weinheim: Wiley John & sons; 1993. p 1-41.
9. Zahringer U, Lindner B, Rietschel ET. Molecular structure of lipid A, the endotoxic center of bacterial lipopolysaccharides. Adv Carbohydr Chem Biochem 1994; 50: 211-76.
10. Kastowsky M, Obst S, Bradaczek H. Molecular dynamics simulations of six different fully hydrated monomeric conformers of *Escherichia coli* re-lipopolysaccharide in the presence and absence of Ca^{2+}. Biophys J 1997; 72: 1031-46.
11. Wang Y, Hollingsworth RI. An NMR spectroscopy and molecular mechanics study of the molecular basis for the supramolecular structure of lipopolysaccharides. Biochem 1996; 35: 5647-54.
12. Pristovsek P, Kidric J. Solution structure of polymyxins B and E and effect of binding to lipopolysaccharide: An NMR and molecular modeling study. J Med Chem 1999; 42: 4604-13.
13. Bhattacharjia D, Mathan B. Polymyxin B nonapeptide: Conformation in water and in lipopolysaccharide-bound state determinated by two dimensional NMR and molecular dynamics. Biopolymers 1997; 41: 251-65.
14. Yin N, Marshall RL, Matheson S, Savage PB. Synthesis of lipid A derivatives and their interactions with polymyxin B and polymyxin B nonapeptide. J Am Chem Soc 2003; 125: 2426-35.
15. Din ZZ, Mukerjee P, Kastowsky M, Takayama K. Effect of pH on solubility and ionic state of lipopolysaccharide obtained from the deep rough mutant of *Escherichia coli*. Biochemistry 1993; 32: 4579-86.
16. Gasteiger J, Marsili M. Iterative partial equalization of orbital electronegativity – a rapid access to atomic charges. Tetrahedron 1980; 36: 3219-22.
17. Brandenburg K, Jurgens G, Andra J, Lindner B, Koch MH, Blume A, Garidel P. Biophysical characterization of the interaction of high-density lipoprotein (HDL) with endotoxins. Eur J Biochem 1988; 269: 5972-81.
18. Dammer U, Hegner M, Anselmetti D, Wagner P, Dreier M, Huber W, Guntherodt HJ. Specific antigen/antibody interactions measured by force microscopy. Biophys J 1996; 70: 2437-41.
19. Dammer U, Popescu O, Wagner P, Anselmetti D, Güntherodt HJ, Misevic NC. Binding strength between cell adhesion proteoglycans measured by atomic force microscopy. Science 1995; 267: 1173-5.
20. Vinckier A, Gervasoni P, Zaugg F, Ziegler U, Lindner P, Groscurth P, Pluckthun A, Semenza G. Atomic force microscopy detects changes in the interaction forces between GroEL and substrate proteins. Biophys J 1998; 74: 3256-63.